Desalination and Water Treatment
www.deswater.com

doi: 10.5004/dwt.2021.27510

231 (2021) 398–406
August

Preparation of magnetic carboxymethyl starch/graphene oxide hydrogel for adsorption of methylene blue

Xiaodong Jiang, Jiankun Wang*, Jing Guo

School of Textile Science and Engineering, TIANGONG UNIVERSITY, Tianjin 300387, China, email: jiankunwang@tiangong.edu.cn (J. Wang)

Received 26 February 2021; Accepted 11 May 2021

ABSTRACT

The magnetic composite hydrogel was prepared by using graphene oxide (GO), carboxymethyl starch (CMS) and Fe_3O_4 as raw materials via a facile one-step reaction route. Magnetic CMS/GO hydrogel was applied as an adsorbent for methylene blue (MB) and characterized by scanning electron microscopy, X-ray diffraction, Fourier-transform infrared spectroscopy, thermogravimetry and vibrating sample magnetometer. Kinetics, isotherm and thermodynamics of adsorption were investigated. The results show that the adsorption of MB onto the hydrogel was well-described by pseudo-second-order adsorption kinetic and Langmuir models, and it was a spontaneous thermal reaction. GO was uniformly dispersed in the hydrogel, which significantly improved the adsorption capacity and thermal stability of the hydrogel. In addition, the adsorbent showed high efficiency for the removal of MB with the maximum adsorption capacity of 622.71 mg/g at 293 K, and its removal efficiency had no significant reduction after five cycles of adsorption. Thus, magnetic CMS/GO hydrogel may be a promising adsorbent for the removal of MB from aqueous solutions in environmental pollution treatment.

Keywords: Magnetic composite hydrogel; Graphene oxide; Carboxymethyl starch; Adsorption; Methylene blue

1. Introduction

Dyes are organic colorant compounds that are widely used in many different industries such as textile, paint, plastic, paper and tanning [1–3]. The application of dyes produced a large amount of harmful wastewater, which caused pollution of natural waters and disrupted the balance of the ecosystem [4]. Methylene blue (MB) is one of the thiazine dyes, which is carcinogenic [5]. Excessive ingestion can cause some adverse effects such as nausea, abdominal pain, precordial pain, dizziness, headache and sweating [6]. Thus, the effective treatment of dye wastewater has become an urgent problem to be solved. To date, many different methods such as adsorption [7], chemical precipitation [8], membrane filtration [9], photodegradation [10] and oxidation [11] have been applied to the treatment of dye wastewater. However, adsorption is the most effective method due to its high removal efficiency, simple operation and low cost [12]. There are many adsorbents for the removal of dyes such as activated carbon, activated diatomaceous earth, natural montmorillonite and coal cinder, and good performances have been achieved [13–15]. Therefore, it is very important to prepare efficient adsorbents to remove dyes from water.

With the increasing interest in green and degradable adsorbents, carboxymethyl starch (CMS) has been gradually taken into account [16]. It has a strong adsorption capacity for dyes due to its large number of reactive groups such as carboxyl and hydroxyl groups. However, it is a water-soluble starch and forms a colloidal solution when dissolved in water, making it difficult to use as an adsorbent for the adsorption of pollutants in water [17]. Therefore, the chemical cross-linking modification was opted to improve its

* Corresponding author.

structural stability. Graphene oxide (GO) is a carbonaceous material with a two-dimensional sheet structure [18]. It is a highly potential and efficient adsorbent due to its large number of oxygen-containing functional groups, ultra-high specific surface area and high selective adsorption [19,20]. However, GO is difficult to be separated from the aqueous solution through traditional centrifugation and filtration methods due to the small particle size and good dispersibility in water [21]. Therefore, Fe_3O_4 nanoparticles can be compounded on the surface of GO to obtain a magnetic composite material that can be separated from the aqueous solution with an external magnetic field [22,23]. Currently, GO, CMS and magnetic particles as adsorbents for the adsorption of MB have been reported independently. However, this work is the first to obtain a magnetic hydrogel by dispersing GO and magnetic nanoparticles into the three-dimensional cross-linked network structure of CMS.

In response to the problems of difficult recycling of GO and high water solubility of CMS, magnetic CMS/GO hydrogel was designed in this paper. Its morphology, structure and thermal stability were characterized. The effects of pH, time, initial dye concentration and adsorbent dosage on the adsorption performance of the composite hydrogel were investigated by using MB as the adsorption model. Kinetics, isotherm and thermodynamics of adsorption were also investigated.

2. Experiment and methods

2.1. Chemicals

Graphite (99.95%) was obtained from Macklin Biochemical Co., Ltd., (Shanghai, China). Carboxymethyl starch (CMS) was bought from Puxiu Biotechnology Co., Ltd., (Hangzhou, China). $FeCl_3{\cdot}6H_2O$ and $FeSO_4{\cdot}7H_2O$ were supplied by Guangfu Technology Development Co., Ltd., (Tianjin, China). Epichlorohydrin (ECH) and methylene blue (MB) were purchased from Kemiou Chemical Reagent Co., Ltd., (Tianjin, China). All other chemicals were of analytical grade.

2.2. Synthesis of hydrogel

2.2.1. Synthesis of GO

GO was prepared from natural graphite using the modified Hummers method [24]. 10 mL H_3PO_4 and 90 mL H_2SO_4 were mixed to obtain a mixed strong acid solution. 0.75 g of graphite powder was dispersed into the mixed solution, and then 4.5 g of potassium permanganate was gradually added to it with stirring at 50°C for 24 h. After the reaction, the mixture cooled to room temperature was carefully poured into 200 mL of ice water containing 2 mL of H_2O_2 and left to stand for 24 h. The substrate was washed to neutral with 1 mol/L HCl and distilled water under 10,000 rpm centrifugation to obtain the graphite oxide dispersion. Then the above dispersion was sonicated for 3 h to obtain a homogeneous graphene oxide solution.

2.2.2. Synthesis of magnetic CMS/GO hydrogel

2 g of CMS, 20 μL of epichlorohydrin, 1 g of $FeSO_4{\cdot}7H_2O$, 2 g of $FeCl_3{\cdot}6H_2O$ were dispersed into 20 mL of GO solution (2 mg/L), and the beaker was placed in a water bath at 70°C and stirred for 30 min. Then 1 mol/L NaOH solution was added to maintain the pH at about 10, and magnetic CMS/GO hydrogel was prepared after 3 h. The hydrogel was immersed in distilled water and washed by renewing the water every 8 h. After repeating three times, the hydrogels were lyophilized using a freeze dryer, and dry-based hydrogels were obtained.

2.3. Characterization

The morphology of the sample was imaged by using scanning electron microscopy (SEM, Phenom XL, Phenom-World, Netherlands) under an accelerating voltage of 10 kV. X-ray diffraction (XRD) patterns were recorded on an X-ray diffractometer (XRD, D8 ADVANCE, Bruker, Germany) using Cu-Kα radiation (λ = 1.5438 Å). The thermal stability was investigated by using a thermogravimetry (TG, 209 F3 Tarsus, NETZSCH-Gerätebau GmbH, Germany) from 50°C to 800°C with a heating rate of 10°C/min under nitrogen atmosphere. The groups of the hydrogel were analyzed by using a Fourier-transform infrared spectroscope (FTIR, Tensor37, Bruker, Germany) at a wavenumber range of 400~4,000 cm^{-1} with a resolution of 4 cm^{-1}. Magnetization measurements were recorded with a vibrating sample magnetometer (Lake Shore 7404, Quantum Design, Inc., USA) with an applied field of between ±30 kOe.

2.4. Dye adsorption

The adsorption properties of hydrogels were investigated using MB as the adsorption object. 5 mg of hydrogel was added to 20 mL of MB solution (50 mg/L) and the mixture was shaken for 100 rpm at 25°C on a constant temperature water bath shaker. The adsorbent was separated from the solution with a magnet and the residual MB solution concentration was measured with a visible spectrophotometer at a wavelength of 664 nm. Finally, removal efficiency (R) and adsorption capacity (q_e) for MB were calculated.

3. Results and discussion

3.1. Synthesis of magnetic CMS/GO hydrogel

CMS is a water-soluble starch with a large number of carboxyl and hydroxyl groups [25]. The hydrogel is prepared by cross-linking between the molecular chains of CMS in the presence of ECH as a crosslinker at the pH value of 10. In addition, Fe_3O_4 particles could also be prepared under this condition, which greatly increases the possibility of preparing magnetic hydrogels by the one-step method. The addition of GO is expected to significantly improve the adsorption properties of the hydrogel due to a large number of reactive groups such as hydroxyl and carboxyl groups, which have strong adsorption on dyes. The schematic illustration for the preparation of magnetic CMS/GO hydrogel is given in Fig. 1. Polymerization was performed in the presence of Fe^{2+}, Fe^{3+} and GO, which is able to homogeneously immobilize the GO flakes and the produced Fe_3O_4 into the polymer network.

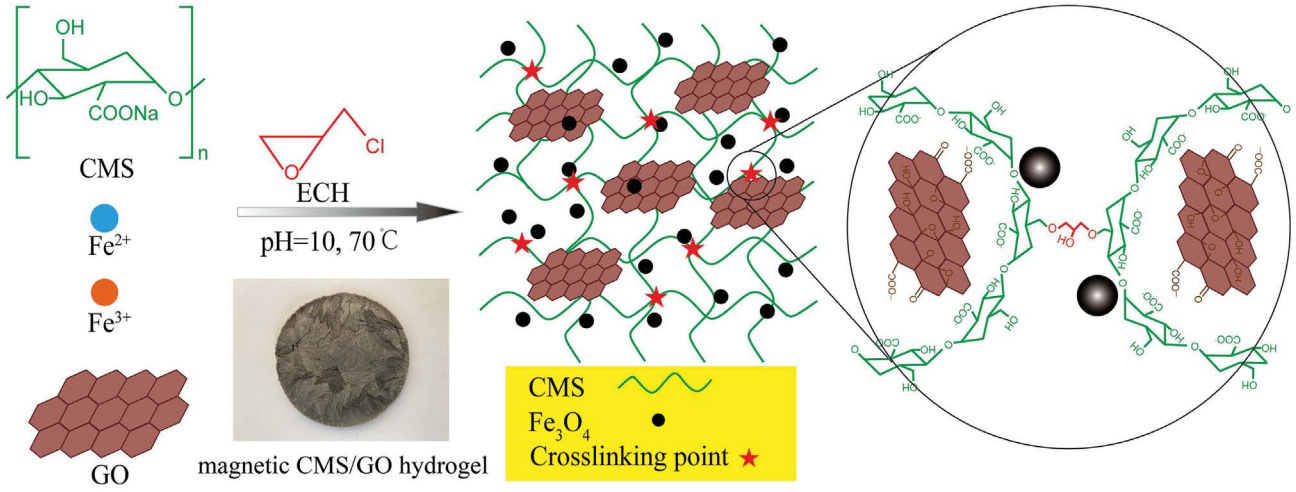

Fig. 1. Schematic illustration for the preparation of magnetic CMS/GO hydrogel.

3.2. Characteristics

The morphology of magnetic CMS/GO hydrogel is shown in Fig. 2. SEM image shows that the hydrogel is porous with interconnected pores that are evenly distributed. This structure can not only increase the specific surface area of the hydrogel but also accelerate the diffusion rate of the dye solution in the polymer network, which significantly increases the diffusion rate of dye molecules and the contact with functional groups. Thus, the adsorption capacity and the adsorption rate of the hydrogel are obviously enhanced.

The XRD patterns of GO and magnetic CMS/GO hydrogel are shown in Fig. 3a. The GO sample has a sharp diffraction peak at 2θ of 10.18° with an interlayer spacing of 0.923 nm, which is much larger than that of natural graphite (0.335 nm) [26]. A large amount of oxygen-containing functional groups was introduced into the sheets of natural graphite, which remarkably increased the interlayer spacing. Since the van der Waals forces between the sheets are greatly reduced by the increase of interlayer spacing, the multilayered GO can be exfoliated into single or few-layered GO by ultrasonic treatment [27]. The hydrogel showed diffraction peaks at 2θ of 30.2°, 35.4°, 43.0°, 57.1°, and 62.6° indexed to (220), (311), (400), (511) and (440), respectively, which corresponded to the crystallographic planes in the Fe_3O_4 crystal structure. This indicates the successful loading of Fe_3O_4 nanoparticles into the composite. In addition, there is no GO diffraction peak at 2θ of 10.18° for GO, indicating that the GO flakes are uniformly embedded in the hydrogel network.

The FTIR spectra of GO and magnetic CMS/GO hydrogel are shown in Fig. 3b. Both samples show a strong peak at 3,250 cm^{-1} which is related to –OH stretching vibration. For GO, the characteristic peaks at 1,730; 1,220 and 1,050 cm^{-1} are associated with –C=O, –C–O–C and –C–O, respectively. For hydrogel, the characteristic peak at 2,925 cm^{-1} is related to –C–H, and the characteristic peak of –C–O–C appears at 1,015–1,150 cm^{-1}, indicating that the CMS crosslinking reaction has occurred. In addition, the characteristic peaks at 697 and 577 cm^{-1} are correlated with Fe–O group,

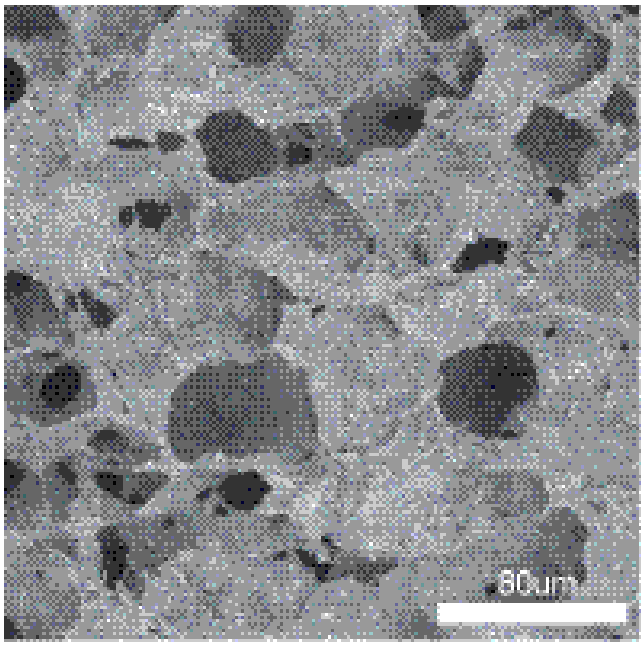

Fig. 2. SEM image of magnetic CMS/GO hydrogel.

which indicates that Fe_3O_4 is successfully compounded with hydrogel [28].

The TG curves of magnetic CMS hydrogel and magnetic CMS/GO hydrogel are shown in Fig. 3c. There was a significant weight loss in both samples. The weight loss of magnetic CMS/GO hydrogel occurred in the range of 255°C to 300°C, while magnetic CMS hydrogel occurred in the range of 262°C to 308°C. In addition, the residual mass of magnetic CMS/GO hydrogel was 44.5%, which was apparently higher than that of magnetic CMS hydrogel at 40.6%. Thus, it indicates that the addition of GO increased the thermal stability of the hydrogel.

Magnetization curves of magnetic CMS/GO hydrogel and the photos of magnetic separation after adsorption are shown in Fig. 3d. Hydrogel exhibits superparamagnetic

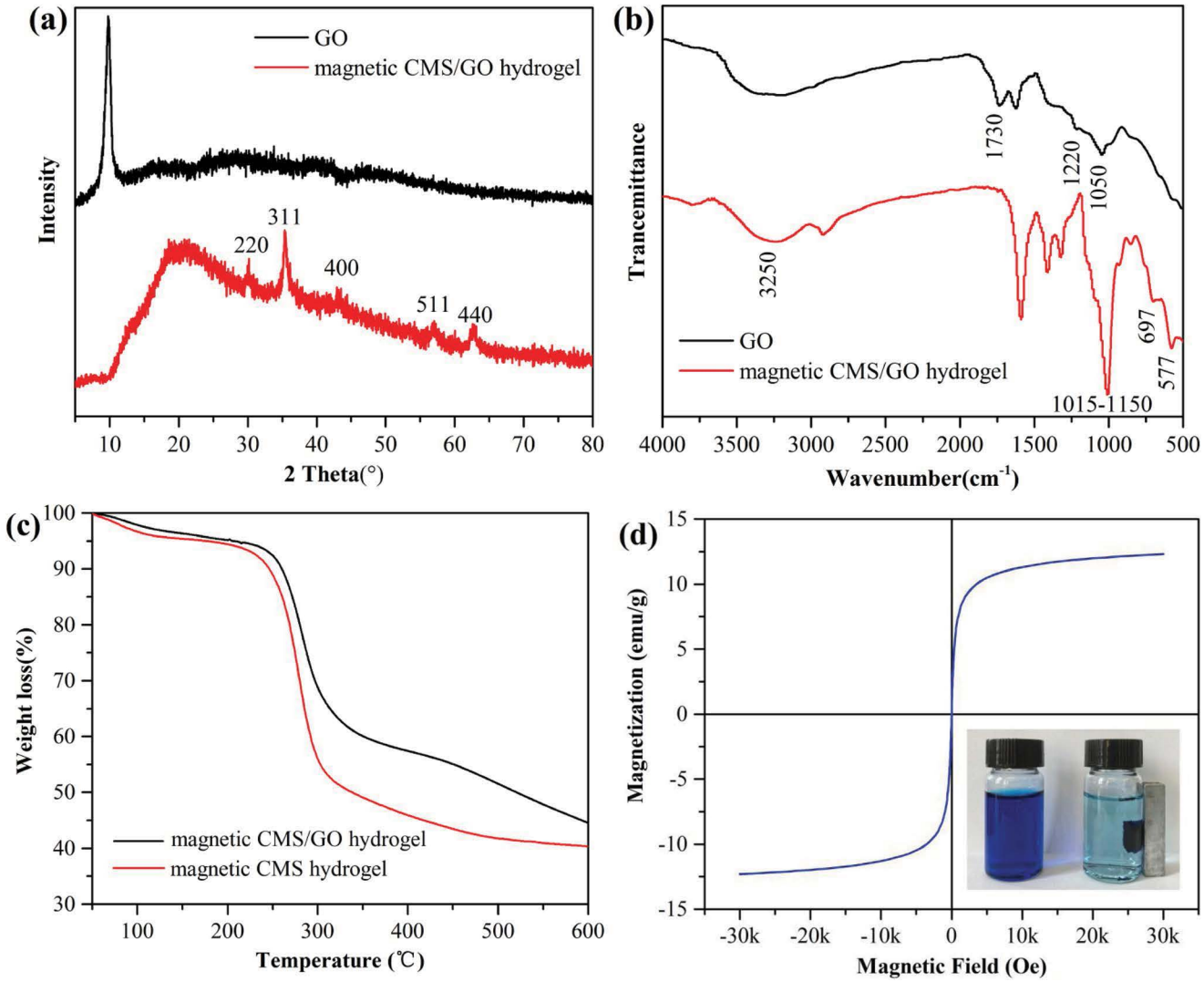

Fig. 3. (a) XRD pattern and (b) FTIR spectra of GO and magnetic CMS/GO hydrogel, (c) TG spectra of magnetic CMS/GO hydrogel and magnetic CMS hydrogel, (d) magnetic hysteresis loop of magnetic CMS/GO hydrogel (The inset shows the magnetic separation of adsorbents from dye solution).

properties at room temperature with a saturation magnetization intensity of 12.30 emu/g. It can be easily separated from the aqueous solution under magnetic action.

3.3. Dye adsorption

3.3.1. Effect of pH

To investigate the effect of pH on dye adsorption, the pH values of MB solutions were adjusted from 3.0 to 11.0 at 20 mL of MB concentration (50 mg/L) and 5.0 mg of adsorbent. As is shown in Fig. 4a, the adsorption capacity of hydrogel increased with increasing pH value and reached the maximum capacity at the pH value of 11.0. It should be due to the fact that the pH values of solution can affect the state of functional groups on the adsorbent and the electrical properties of the dye [29]. In acidic solutions, the competition between the cationic MB and H_3O^+ reduces the chance of binding to the active site of the adsorbent, resulting in a lower adsorption capacity of the hydrogel. In addition, active sites such as –COOH and –OH become negatively charged due to deprotonation at high pH values, which promotes electrostatic interactions between the adsorbent and MB molecules. Therefore, the hydrogel has high adsorption capacity under alkaline conditions.

3.3.2. Effect of initial dye concentration

The adsorption capacity of the hydrogel in MB solutions of different initial concentrations is shown in Fig. 4b. The adsorption capacity of magnetic CMS/GO hydrogel increased from 166.75 to 632.16 mg/g at 393 K as the initial concentration of MB increases from 50 to 250 mg/L. This indicates that the mass gradient was the main driving force for adsorption [30]. In addition, the adsorption capacity increases at a decreasing rate and eventually tends to a constant as MB initial concentration increases.

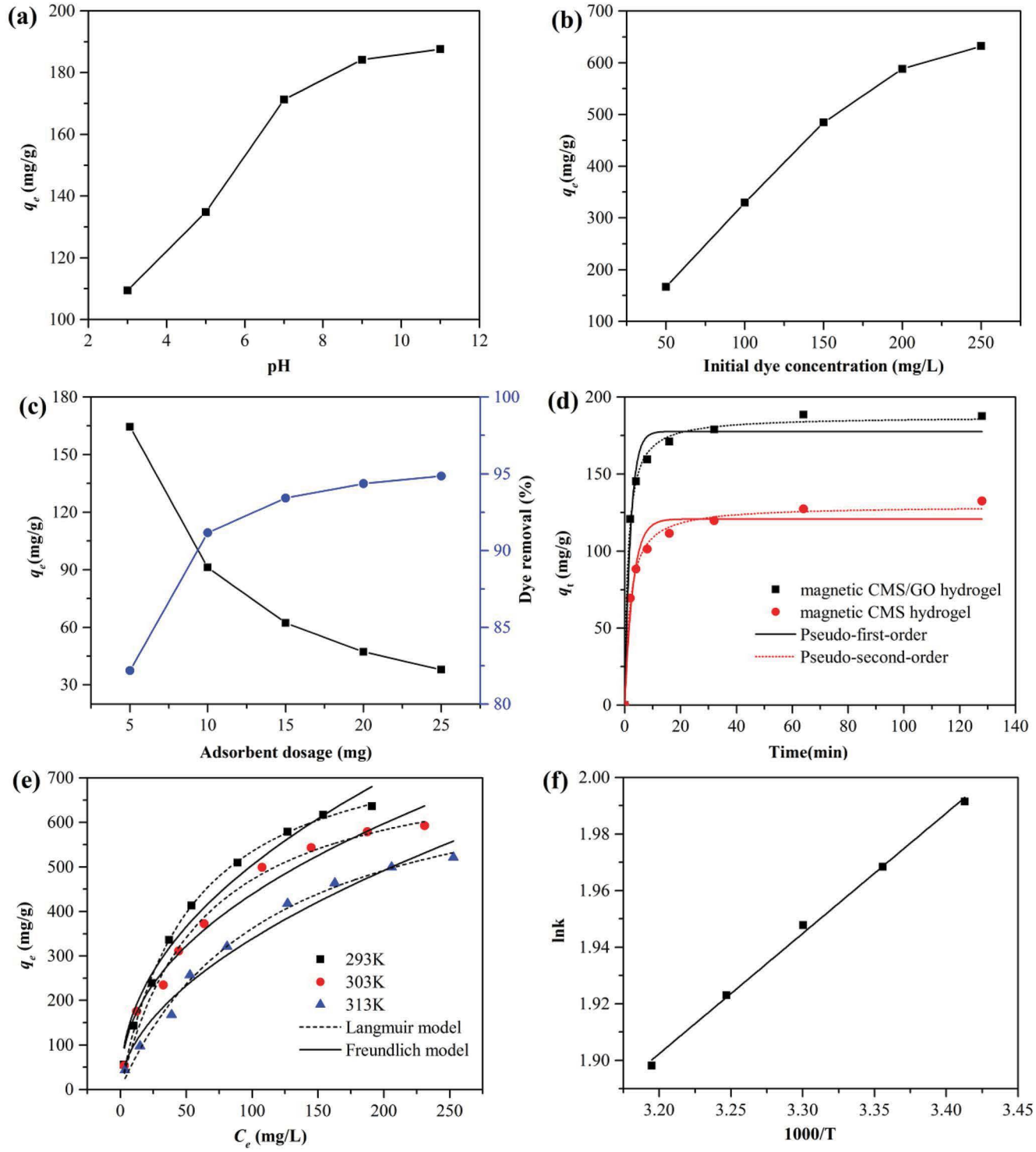

Fig. 4. (a) Effect of initial pH, (b) effect of initial dye concentration, (c) effect of adsorbent dosage on the adsorption capacity of MB onto magnetic CMS/GO hydrogel, (d) effect of contact time with pseudo-first-order and pseudo-second-order non-linear plots of adsorption kinetics for MB onto hydrogels, (e) Langmuir model and Freundlich model non-linear plots of the adsorption isotherm at different temperatures, and (f) the thermodynamic analysis of magnetic CMS/GO hydrogel.

3.3.3. *Effect of adsorbent dosage*

The effects of adsorbent dosage on the adsorption capacity and the rate of dye removal were evaluated by adding a range of 5–25 mg of adsorbent to 20 mL of MB solution (50 mg/L). As is shown in Fig. 4c, the adsorption capacity of the adsorbent significantly decreases from 164.37 to 37.94 mg/g with increasing dosage, while dye removal

increases from 82.18% to 94.85%. This result is related to the splitting effect of the flux or concentration gradient between the dye molecule and the adsorbent [31].

3.3.4. Effect of contact time and adsorption kinetic

The effect of contact time from 0 to 120 min on the adsorption capacity of the hydrogels was examined at MB concentration of 50 mg/L, the dosage of 5.0 mg and temperature 293 K and this result is shown in Fig. 4d. It is clearly seen that the adsorption capacity of the hydrogels increases rapidly in the initial stage. With the increase of contact time, the adsorption capacity increases more and more slowly and finally tends to level off, which is mainly caused by the decrease of MB concentration and adsorption sites. The adsorption capacity of magnetic CMS/GO hydrogel was 187.64 mg/g, which was significantly higher than that of magnetic CMS hydrogel of 132.48 mg/g. Therefore, the addition of GO significantly improved the adsorption capacity of the hydrogel due to its extremely high adsorption capacity.

In order to investigate the adsorption mechanism of hydrogels towards MB, pseudo-first-order and pseudo-second-order adsorption kinetic models were used to fit the experimental data, and their expressions are described as follows, respectively [32]:

$$\log\left(q_e - q_t\right) = \log q_e - \frac{k_1}{2.303}t \tag{1}$$

$$\frac{t}{q_t} = \frac{1}{k_2 q_e^2} + \frac{t}{q_e} \tag{2}$$

where q_e and q_t (mg/g) are the adsorption capacity of MB at equilibrium and time t (min), respectively. k_1 and k_2 are the equilibrium rate constants of the pseudo-first-order and pseudo-second-order adsorption kinetic models, respectively.

Kinetic parameters for the adsorption of MB onto magnetic CMS hydrogel and magnetic CMS/GO hydrogel are shown in Table 1. The correlation coefficient (R^2) of the quasi-second-order kinetic model was significantly higher than that of the quasi-first-order kinetic model, and its predicted value was closer to the experimental value (q_{exp}), indicating that the hydrogel adsorbed MB mainly by chemisorption.

3.3.5. Adsorption isotherm

The adsorption isotherms of magnetic CMS/GO hydrogel were studied by calculating the adsorption capacity in relation to the equilibrium concentration of MB at different temperatures (293, 303 and 313 K). In particular, Langmuir isothermal adsorption model is based on the assumption that the adsorption sites on the adsorbent surface are restricted and uniformly distributed and there is no interaction between adsorbents with the same adsorption force. In contrast, Freundlich isothermal adsorption model is used to describe the adsorption behavior on non-uniform surfaces [33]. Langmuir and Freundlich isothermal adsorption models were used to investigate the interaction of dyes with the adsorbent and the non-linear forms are expressed as follows [34]:

$$\frac{1}{q_e} = \frac{1}{C_e K_L q_m} + \frac{1}{q_m} \tag{3}$$

$$\log q_e = \log K_F + \frac{1}{n}\log C_e \tag{4}$$

where C_e is dye equilibrium concentration (mg/g), K_L is Langmuir adsorption constant, q_e is adsorption capacity of MB at equilibrium (mg/g), q_m is maximum adsorption capacity (mg/g). K_F is Freundlich constant and n is heterogeneity factor.

Fig. 4e displays that a lower temperature is more beneficial for the adsorption of MB into magnetic CMS/GO hydrogel. This may be related to the weakening of the interaction between the active site of adsorbent and MB molecules with increasing temperature [35]. In addition, the adsorption capacity of the adsorbent gradually increases with increasing adsorption equilibrium concentration of MB and finally tends to equilibrium. The nonlinear fitting parameters of Langmuir and Freundlich's isothermal models are shown in Table 2. It is obvious that the R^2 of the Langmuir isotherm model is significantly higher than that of the Freundlich isotherm model, which indicates that adsorption is well-described by the Langmuir isotherm model.

Table 2
Constants and correlation coefficients of Langmuir and Freundlich models for MB adsorption onto magnetic CMS/GO hydrogel at different temperatures

T (K)	Langmuir			Freundlich		
	q_m (mg/g)	K_L	R^2	K_F	n	R^2
293	622.71	0.0326	0.989	82.562	2.742	0.940
303	609.67	0.0239	0.982	66.056	2.572	0.953
313	586.84	0.0177	0.992	48.282	2.339	0.961

Table 1
Kinetic parameters for the adsorption of MB onto adsorbents

		Pseudo-first-order			Pseudo-second-order		
Adsorbent	q_{exp} (mg/g)	k_1 (min^{-1})	q_e (mg/g)	R^2	k_2 (min^{-1})	q_e (mg/g)	R^2
Magnetic CMS	187.64	0.4955	177.67	0.973	0.0046	187.28	0.997
Magnetic CMS/GO	132.48	0.3471	120.75	0.956	0.0041	129.36	0.994

3.3.6. Adsorption thermodynamics

In order to further analyze the effect of temperature on the adsorption process of magnetic CMS/GO hydrogel, the adsorption process was tested at five different temperatures (293, 298, 303, 308, 313 K). The thermodynamic parameters such as Gibbs free energy (ΔG°), entropy (Δ*H*°) and enthalpy (Δ*S*°) are calculated by the following equations [36].

$$\ln K_d = \frac{\Delta S^\circ}{R} - \frac{\Delta H^\circ}{RT} \quad (5)$$

$$\Delta G^\circ = \Delta H^\circ - T\Delta S^\circ \quad (6)$$

where K_d is produced by q_e/C_e. T is the absolute temperature in Kelvin, Δ*S*° is the entropy change, Δ*H*° is the enthalpy constant, and R is the universal gas constant [8.314 J/(mol K)]. The values of Δ*H*° and Δ*S*° were calculated by the slope and intercept of linear fitting in Fig. 4f.

The thermodynamic parameters were calculated as shown in Table 3. The value of ΔG° increased from 5.042 to 5.651 as the temperature increases from 293 to 313 K. This result demonstrates that the adsorption process of MB by the adsorbent is a spontaneous reaction. In addition, the value of Δ*H*° is negative, indicating the adsorption is an exothermic reaction. Furthermore, the value of Δ*S*° is positive, illustrating an increase in the randomness of the solid/solution interface.

3.4. Desorption and reusability evaluation

In order to investigate the repeatability, magnetic CMS/GO hydrogel was desorbed by stirring in 70% ethanol solution for 3 h and dried at 40°C. The dye removal efficiency of the hydrogel after five adsorption–desorption treatments is shown in Fig. 5. It can be clearly seen that the removal efficiency of the hydrogel remains above 90% after 5 times of recycling, indicating that the hydrogel has excellent reproducibility. In addition, the hydrogel can be easily separated from the wastewater by using a magnet due to its stable magnetic properties. Therefore, hydrogels can be used as ideal adsorbents for the treatment of dye wastewater.

3.5. Comparison with other adsorbents

In order to further understand the adsorption ability of magnetic CMS/GO hydrogel, the results of the adsorbent were compared with other adsorbents for the adsorption capacity of MB. The maximum adsorption capacity and conditions of the various adsorbents are shown in Table 4. It can be seen that magnetic CMS/GO hydrogel adsorbents show a much higher adsorption capacity for MB than other adsorbents. In addition, the hydrogel is an ideal and

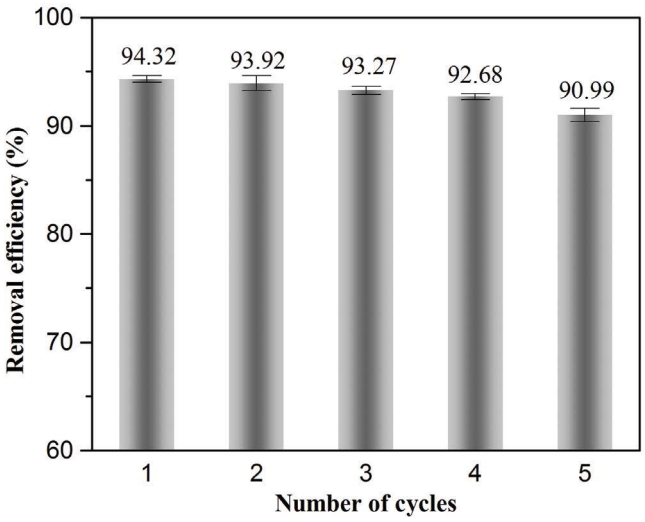

Fig. 5. Reusability of magnetic CMS/GO hydrogel.

Table 3
Thermodynamic analysis data for the adsorption of MB onto magnetic CMS/GO hydrogel (R^2 = 0.9963)

Δ*H*° (kJ/mol)	Δ*S*° (J/K mol)	ΔG° (kJ/mol)				
		293.15 K	298.15 K	303.15 K	308.15 K	313.15 K
–3.54	4.49	–5.042	–5.191	–5.345	–5.492	–5.651

Table 4
Comparison with other adsorbents

Adsorbent	Contact time (h)	q_m (mg/g)	pH	Reference
Activated carbon	5	270.27	6	[37]
Cellulose nanocrystal	4	217.4	7	[38]
Magnetic chitosan/GO composite	1.5	95.16	5.3	[39]
Magnetic xylan/poly(acrylic acid) hydrogel	1	438.60	8	[40]
Carbon/montmorillonite composite	6	138.1	8	[41]
Magnetic chitosan composite	24	45.1	5.5	[42]
Magnetic CMS/GO hydrogel	2	622.71	7	This study

efficient adsorbent due to its high adsorption rates and moderate conditions.

4. Conclusion

In this study, a magnetic GO/CMS hydrogel was successfully synthesized and used as an adsorbent for the removal of MB from aqueous solutions. The hydrogel has excellent adsorption performance with an adsorption capacity of up to 622.71 mg/L for MB. The results show that the addition of GO can significantly enhance the adsorption capacity and thermal stability of the hydrogel. The hydrogel has good magnetic separation and can be easily separated and recovered from the wastewater under the action of an applied magnetic field. Moreover, the hydrogel has good reusability and no significant decrease in adsorption efficiency after multiple reuses. Thus, magnetic GO/CMS hydrogel has potential application prospects for the removal of MB in dye wastewater.

References

[1] D.R. Waring, G. Hallas, The Chemistry and Application of Dyes, Springer Science & Business Media, New York, 2013.
[2] U. Shanker, M. Rani, V. Jassal, Degradation of hazardous organic dyes in water by nanomaterials, Environ. Chem. Lett., 15 (2017) 623–642.
[3] R.W. Sabnis, Developments in the chemistry and applications of phthalein dyes. Part 1: industrial applications, Color. Technol., 134 (2018) 187–205.
[4] L.-L. Jiang, K. Li, D.-L. Yang, M.-F. Yang, L. Ma, L.-Z. Xie, Toxicity assessment of 4 azo dyes in Zebrafish embryos, Int. J. Toxicol., 39 (2020) 115–123.
[5] S. Soni, P.K. Bajpai, J. Mittal, C. Arora, Utilisation of cobalt doped Iron based MOF for enhanced removal and recovery of methylene blue dye from waste water, J. Mol. Liq., 314 (2020) 113642, doi: 10.1016/j.molliq.2020.113642.
[6] K. Polat, E.A. Bursalı, A promising strategy for the utilization of waste nitrile gloves: cost-effective adsorbent synthesis, J. Mater. Cycles Waste, 21 (2019) 659–665.
[7] M. Naushad, A.A. Ansari, Z.A. ALOthman, J. Mittal, Synthesis and characterization of YVO_4:Eu^{3+} nanoparticles: kinetics and isotherm studies for the removal of Cd^{2+} metal ion, Desal. Water Treat., 57 (2014) 2081–2088.
[8] H. Kono, R. Kusumoto, Removal of anionic dyes in aqueous solution by flocculation with cellulose ampholytes, J. Water Process Eng., 7 (2015) 83–93.
[9] C.Z. Liang, S.P. Sun, F.Y. Li, Y.K. Ong, T.S. Chung, Treatment of highly concentrated wastewater containing multiple synthetic dyes by a combined process of coagulation/flocculation and nanofiltration, J. Membr. Sci., 469 (2014) 306–315.
[10] H.R. Rashidi, N.M.N. Sulaiman, N.A. Hashim, Synthetic reactive dye wastewater treatment by using nano- membrane filtration, Desal. Water Treat., 55 (2015) 86–95.
[11] Y.-H. Chiu, T.-F.M. Chang, C.-Y. Chen, M. Sone, Y.-J. Hsu, Mechanistic insights into photodegradation of organic dyes using heterostructure photocatalysts, Catalysts, 9 (2019) 430, doi: 10.3390/catal9050430.
[12] K.B. Tan, M. Vakili, B.A. Horri, P.E. Poh, A.Z. Abdullah, B. Salamatinia, Adsorption of dyes by nanomaterials: recent developments and adsorption mechanisms, Sep. Purif. Technol., 150 (2015) 229–242.
[13] C. Arora, P. Kumar, S. Soni, J. Mittal, A. Mittal, B. Singh, Efficient removal of malachite green dye from aqueous solution using *Curcuma caesia* based activated carbon, Desal. Water Treat., 195 (2020) 341–352.
[14] J.X. Lin, S.L. Zhan, M.H. Fang, X.Q. Qian, The adsorption of dyes from aqueous solution using diatomite, J. Porous Mater., 14 (2007) 449–455.
[15] P. Huang, A. Kazlauciunas, R. Menzel, L. Lin, Determining the mechanism and efficiency of industrial dye adsorption through facile structural control of organo-montmorillonite adsorbents, ACS Appl. Mater. Interaces, 9 (2017) 26383–26391.
[16] G. Gong, F. Zhang, Z. Cheng, L. Zhou, Facile fabrication of magnetic carboxymethyl starch/poly(vinyl alcohol) composite gel for methylene blue removal, Int. J. Biol. Macromol., 81 (2015) 205–211.
[17] L. Chen, H. Hao, W. Zhang, Z. Shao, Adsorption mechanism of copper ions in aqueous solution by chitosan-carboxymethyl starch composites, J. Appl. Polym. Sci., 137 (2020) 48636, doi: 10.1002/app.48636.
[18] D.C. Marcano, D.V. Kosynkin, J.M. Berlin, A. Sinitskii, Z.Z. Sun, A. Slesarev, L.B. Alemany, W. Lu, J.M. Tour, Improved synthesis of graphene oxide, ACS Nano, 4 (2010) 4806–4814.
[19] K. Erickson, R. Erni, Z. Lee, N. Alem, W. Gannett, A. Zettl, Determination of the local chemical structure of graphene oxide and reduced graphene oxide, Adv. Mater., 22 (2010) 4467–4472.
[20] A. Molla, Y. Li, B. Mandal, S.G. Kang, S.H. Hur, J.S. Chung, Selective adsorption of organic dyes on graphene oxide: theoretical and experimental analysis, Appl. Surf. Sci., 464 (2019) 170–177.
[21] S. Song, Y. Ma, H. Shen, M. Zhang, Z. Zhang, Removal and recycling of ppm levels of methylene blue from an aqueous solution with graphene oxide, RSC Adv., 5 (2015) 27922–27932.
[22] N.H. Othman, N.H. Alias, M.Z. Shahruddin, N.F.A. Bakar, N.R.N. Him, W.J. Lau, Shahruddin, Adsorption kinetics of methylene blue dyes onto magnetic graphene oxide, J. Environ. Chem. Eng., 6 (2018) 2803–2811.
[23] S. Bai, X. Shen, X. Zhong, Y. Liu, G. Zhu, X. Xu, K. Chen, One-pot solvothermal preparation of magnetic reduced graphene oxide-ferrite hybrids for organic dye removal, Carbon, 50 (2012) 2337–2346.
[24] J.F. Shen, Y.Z. Hu, M. Shi, X. Liu, C. Qin, C. Li, M.X. Ye, Fast and facile preparation of graphene oxide and reduced graphene oxide nanoplatelets, Chem. Mater., 21 (2009) 3514–3520.
[25] Y.X. Chen, G.Y., Wang, Adsorption properties of oxidized carboxymethyl starch and cross-linked carboxymethyl starch for calcium ion, Colloids Surf., A, 289 (2006) 75–83.
[26] Y. Zhu, S. Murali, W. Cai, X. Li, J.W. Suk, J.R. Potts, R.S. Ruoff, Graphene and graphene oxide: synthesis, properties, and applications, Adv. Mater., 22 (2010) 3906–3924.
[27] A.M. Dimiev, J.M. Tour, Mechanism of graphene oxide formation, ACS Nano, 8 (2014) 3060–3068.
[28] S.M. Mousavi, S.A. Hashemi, A.M. Amani, H. Esmaeili, Y. Ghasemi, A. Babapoor, F. Mojoudi, O. Arjomand, Pb(II) removal from synthetic wastewater using Kombucha Scoby and graphene oxide/Fe_3O_4, Physical Chemistry Research, 6 (2018) 759–771.
[29] S. Das, P. Chakraborty, R. Ghosh, S. Pau, S. Mondal, A. Panja, A.K. Nandi, Folic acid-polyaniline hybrid hydrogel for adsorption/reduction of chromium(VI) and selective adsorption of anionic dye from water, ACS Sustainable Chem. Eng., 5 (2017) 9325–9337.
[30] N.A. Fakhre, B.M. Ibrahim, The use of new chemically modified cellulose for heavy metal ion adsorption, J. Hazard. Mater., 343 (2018) 324–331.
[31] M. Haroon, L. Wang, H. Yu, R.S. Ullah, R.U. Khan, Q. Chen, J. Liu, Synthesis of carboxymethyl starch-g-polyvinylpyrolidones and their properties for the adsorption of Rhodamine 6G and ammonia, Carbohydr. Polym., 186 (2018) 150–158.
[32] A. Pourjavadi, M. Nazari, S.H. Hosseini, Synthesis of magnetic graphene oxide-containing nanocomposite hydrogels for adsorption of crystal violet from aqueous solution, RSC Adv., 5 (2015) 32263–32271.
[33] D. Zhao, X. Gao, C. Wu, R. Xie, S. Feng, C. Chen, Facile preparation of amino functionalized graphene oxide decorated with Fe_3O_4 nanoparticles for the adsorption of Cr(VI), Appl. Surf. Sci., 384 (2016) 1–9.
[34] G.A. Mahmoud, S.F. Mohamed, H.M. Hassan, Removal of methylene blue dye using biodegradable hydrogel and reusing in a secondary adsorption process, Desal. Water Treat., 54 (2015) 2765–2776.

[35] Q. Peng, M. Liu, J. Zheng, C. Zhou, Adsorption of dyes in aqueous solutions by chitosan-halloysite nanotubes composite hydrogel beads, Microporous Mesoporous Mater., 201 (2015) 190–201.
[36] Z. Zhao, X. Wang, J. Qiu, J. Lin, D. Xu, C. Zhang, Three-dimensional graphene-based hydrogel/aerogel materials, Rev. Adv. Mater. Sci., 36 (2014) 137–151.
[37] Y. Li, Q. Du, T. Liu, X. Peng, J. Wang, J. Sun, Y. Wang, S. Wu, Z. Wang, Y. Xia, L. Xia, Comparative study of methylene blue dye adsorption onto activated carbon, graphene oxide, and carbon nanotubes, Chem. Eng. Res. Des., 91 (2013) 361–368.
[38] X. Yang, H. Liu, F. Han, S. Jiang, L. Liu, Z. Xia, Fabrication of cellulose nanocrystal from *Carex meyeriana* Kunth and its application in the adsorption of methylene blue, Carbohydr. Polym., 175 (2017) 464–472.
[39] L. Fan, C. Luo, X. Li, F. Lu, H. Qiu, M. Sun, Fabrication of novel magnetic chitosan grafted with graphene oxide to enhance adsorption properties for methyl blue, J. Hazard. Mater., 215 (2012) 272–279.
[40] X.F. Sun, B. Liu, Z. Jing, H. Wang, Preparation and adsorption property of xylan/poly(acrylic acid) magnetic nanocomposite hydrogel adsorbent, Carbohydr. Polym., 118 (2015) 16–23.
[41] D.S. Tong, C.W. Wu, M.O. Adebajo, G.C. Jin, W.H. Yu, S.F. Ji, C.H. Zhou, Adsorption of methylene blue from aqueous solution onto porous cellulose-derived carbon/montmorillonite nanocomposites, Appl. Clay Sci., 161 (2018) 256–264.
[42] D.W. Cho, B.H. Jeon, C.M. Chon, F.W. Schwartz, Y. Jeong, H. Song, Magnetic chitosan composite for adsorption of cationic and anionic dyes in aqueous solution, J. Ind. Eng. Chem., 28 (2015) 60–66.